

## BRIEF COMMUNICATION

Structure of Two-Dimensional Conductor of  $\text{Sr}_2\text{RhO}_4$ 

Mitsuru Itoh,\* Tetsuo Shimura,\* Yoshiyuki Inaguma,\* and Yukio Morii†

\*Research Laboratory of Engineering Materials, Tokyo Institute of Technology, 4259 Nagatsuta, Midori-ku, Yokohama 227, Japan; and  
†Japan Atomic Energy Institute, Tokai-mura, Naka-gun, Ibaraki 319-11, Japan

Received February 1, 1995; accepted March 6, 1995

The structure of the two-dimensional conductor  $\text{Sr}_2\text{RhO}_4$  was refined by powder X-ray diffraction analysis at room temperature.  $\text{Sr}_2\text{RhO}_4$  crystallizes with the symmetry of space group  $I4_1/acd$  (No. 142-2), isostructural with  $\text{Sr}_2\text{IrO}_4$ , and the room temperature lattice parameter  $a = 0.54516(1)$  nm and  $c = 2.57539(4)$  nm. The rotating angle of  $\text{RhO}_6$  octahedra about the  $c$  axis is  $10^\circ$ . The structural data was found to be almost same as that for semiconducting and antiferromagnetic  $\text{Sr}_2\text{IrO}_4$ . © 1995 Academic Press, Inc.

Recently, many studies on  $3d$  transition metal oxides have been carried out for the purpose of finding new superconductors. According to the ligand field theory,  $3d$  transition metals in the sixfold coordination site can occur in both high-spin and low-spin states, while  $4d$  and  $5d$  transition metals tend to take the low-spin state. It is of interest whether we can obtain a new metallic conductor containing  $4d$  and  $5d$  transition metals. Some of our previous studies (1-4) are focused on the development of new metallic conductors containing platinum-group metals. Semiconducting  $\text{LaRhO}_3$  with low-spin  $\text{Rh}^{3+}$  ( $t_{2g}^6$ ; ground term  $^1A_{1g}$ ) can be doped with holes in the  $t_{2g}$  band by the substitution of  $\text{Ca}^{2+}$ ,  $\text{Sr}^{2+}$ , and  $\text{Ba}^{2+}$  for  $\text{La}^{3+}$  (2). By this substitution conductivity increased about three orders of magnitude at room temperature. On the contrary, semiconducting two-dimensional  $\text{SrLaRhO}_4$  with low-spin  $\text{Rh}^{3+}$  was doped with holes by a change in the Sr/La ratio (4). The positive temperature coefficient of resistivity was confirmed in the range  $0.0 < x \leq 0.15$  in  $\text{Sr}_{2-x}\text{La}_x\text{RhO}_4$ ; however, the absolute value of the resistivity was fairly large, larger than  $10^2$  mΩcm. This is the second example of the appearance of metallic conductivity in the  $4d$  and  $5d$  transition-metal oxides with  $\text{K}_2\text{NiF}_4$  structure, the first compound having been  $\text{Sr}_2\text{RuO}_4$  (5) with a  $4d^4$  configuration. Quite recently, Crawford *et al.* (6) reported that  $\text{Sr}_2\text{IrO}_4$  with low-spin  $\text{Ir}^{4+}$  ( $t_{2g}^5$ ; ground term  $^2T_2$ ) crystallizes with the symmetry  $I4_1/acd$  (No. 142-2) instead of  $I4/mmm$ , as determined by the powder neutron diffraction

technique. In this structure,  $\text{IrO}_6$  octahedra are rotated about the crystallographic  $c$  axis by about  $10.5^\circ$ . In our previous report on the structure of  $\text{Sr}_2\text{RhO}_4$  (4), the orthorhombic space group  $Cmca$  or  $Fmmm$  was assigned to explain the additional superreflection lines, due to superstructures other than the  $I4/mmm$  space group. In this case, almost all the peaks were explained by considering the orthorhombic symmetry, but some of very small superreflection lines could not be explained using these space groups.

In this paper, we have reexamined the structure of  $\text{Sr}_2\text{RhO}_4$  by the powder X-ray diffraction technique.

$\text{Sr}_2\text{RhO}_4$  was prepared by the conventional solid state reaction technique. Stoichiometric amounts of  $\text{SrCO}_3$  (99.9%) and  $\text{La}_2\text{O}_3$  (99.9%) were mixed in an agate mortar with ethanol. The dried mixture was pressed into a pellet 1 mm thick and 12 mm in diameter, under a static pressure of about 80 MPa. The pellet was cooled to room temperature and reground in an agate mortar, followed by mixing and pelletization. This pellet was sintered at 1523 K for 36 h in an  $\text{O}_2$  gas flow. Phase characterization and determination of the lattice parameter were carried out using a Mac Science MXP18 powder X-ray diffractometer equipped with a graphite monochromator. The experimental conditions were: accelerating voltage, 50 kV; current, 300 mA; and Cu target. The data were collected by accumulating counts for 1 s in the range  $2\theta = 20^\circ$  to  $120^\circ$ . The crystal structure of the sample was analyzed using the Rietveld analysis program, RIETAN (7).

Figure 1 shows the results of the powder X-ray diffraction measurement, together with the Rietveld refinement and difference plot at 293 K. The inset shows the enlarged part between  $35^\circ$  and  $39^\circ$ . Reflection lines (211) and (213) originate from the superstructure with dimensions of  $2c$  and  $\sqrt{2}a$ , compared with the primitive cell of the  $\text{K}_2\text{NiF}_4$  structure. Other additional feasible peaks due to the superstructure were not observable by the X-ray diffraction technique. Crawford *et al.* (6) used the complete ordered

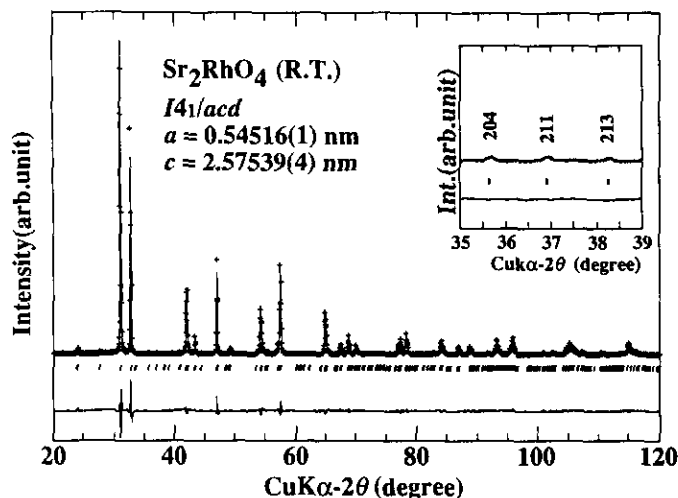


FIG. 1. Powder X-ray diffraction pattern and Rietveld refinement for  $\text{Sr}_2\text{RhO}_4$  at 293 K. The crosses are the data, the solid line is the fitted pattern, the vertical markers indicate expected peak positions, and the residuals appear at the bottom of the figure. The inset shows the enlarged portion between  $35^\circ$  and  $39^\circ$ .

model of the rotation of  $\text{IrO}_6$  octahedra about the  $c$  axis for  $\text{Sr}_2\text{IrO}_4$  with the space group  $I4_1/acd$ , which is the same for  $\text{Ca}_2\text{MnO}_4$  (8). The refinement using the space group  $I4_1/acd$  yielded the  $R$  values,  $R_{\text{wp}} = 13.19\%$ ,  $R_p = 9.39\%$ ,  $R_R = 11.39\%$ ,  $R_E = 3.46\%$ ,  $R_1 = 3.19\%$ , and  $R_F = 3.43\%$ . Huang *et al.* (9) applied the partial disordered model in the rotation of  $\text{IrO}_6$  octahedra. In the ordered structure, the arrangement of the oxygen atoms obeys the symmetry requirements of the screw axis  $4_1$  parallel to  $c$  axis. On the contrary, in the disordered model an uncorrelated rotation of the  $\text{IrO}_6$  octahedra with respect to the

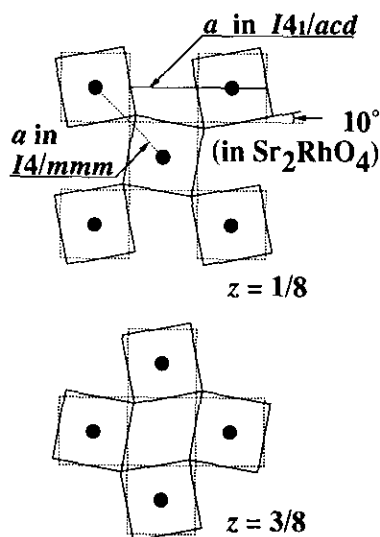


FIG. 2. Structure diagram of  $\text{Sr}_2\text{RhO}_4$  with  $I4_1/acd$  space group, showing the  $\text{RhO}_6$  octahedra rotation at  $z = 1/8$  and  $z = 3/8$ . The broken lines show the primitive  $\text{K}_2\text{NiF}_4$  structure.

TABLE 1  
Crystallographic Information for  $\text{Sr}_2\text{RhO}_4$  at Room Temperature

Lattice parameters (nm)		
$a$		0.54516(1)
$c$		2.57538(4)
Atomic positions and isotropic thermal parameters ( $\text{nm}^2$ )		
Sr(16d)	$z$	0.5511(1)
	$B$	0.0060(9)
Rh(8a)	$B$	0.0029(9)
O1(16d)	$z$	0.455(1)
	$B$	0.007(5)
O2(a)(16f)	$x$	0.294(7)
	$B$	0.002(7)
	$g$	0.12(9)
O2(b)(16f)	$x$	0.206(7)
	$B$	0.002(7)
	$g$	0.88(9)
Bond distance (nm) and angles (degree)		
Rh-O1	(X2)	0.205(2)
Rh-O2	(X4)	0.1957(6)
Sr-O1	(X1)	0.248(3)
Sr-O1	(X4)	0.2730(1)
Sr-O2	(X2)	0.248(2)
Sr-O2	(X2)	0.296(2)
Rh-O2-Rh		160(2)
Rh-O1-Sr		86.8(5)
$R_{\text{wp}}$		13.17%
$R_p$		9.34%
$R_R$		11.35%
$R_E$		3.46%
$R_1$		2.85%
$R_F$		2.75%

Note. The structure was refined in the tetragonal space group  $I4_1/acd$ . The five unique atoms have the following positions: Sr, (0, 0.25,  $z$ ); Rh, (0, 0.25, 0.375); O1, (0, 0.25,  $z$ ); O2(a), ( $x$ ,  $x + 0.25$ , 0.125); O2(b); ( $x$ ,  $x + 0.25$ , 0.125).

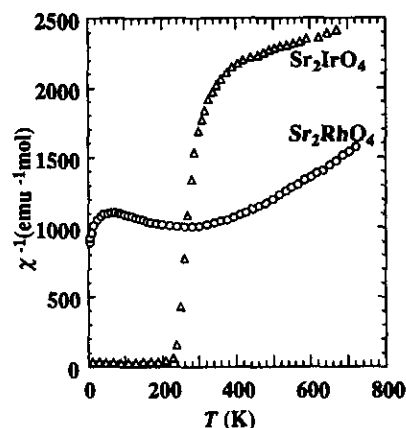


FIG. 3. Temperature dependence of the reciprocal magnetic susceptibilities for  $\text{Sr}_2\text{RhO}_4$  and  $\text{Sr}_2\text{IrO}_4$ .

TABLE 2  
Comparison of the Crystallographic Parameters for  $\text{Sr}_2\text{RhO}_4$ ,  $\text{Sr}_2\text{RuO}_4$ [12], and  $\text{Sr}_2\text{IrO}_4$ [13]

Compound	$a/\text{nm}$	$c/\text{nm}$	Space group	$d_{\text{M-O}}/\text{nm}$ ( $a$ axis)	$d_{\text{M-O}}/\text{nm}$ ( $c$ axis)	$d_{\text{M-O}(c)}/d_{\text{M-O}(a)}$	Rotating angle of $\text{MO}_6$
$\text{Sr}_2\text{RhO}_4$	0.54516(1)	2.57539(4)	$I4_1/acd$	0.1953(5)	0.205(2)	1.049	$10^\circ$
$\text{Sr}_2\text{IrO}_4$	0.549556(7)	2.57933(5)	$I4_1/acd$	0.1977(3)	0.2058(1)	1.041	$10.5^\circ$
$\text{Sr}_2\text{RuO}_4$	0.3871(1)	1.2702(4)	$I4/mmm$	0.19355(4)	0.2071(19)	1.070	$0^\circ$
	0.5474(2) <sup>a</sup>	2.5404(8) <sup>b</sup>					

<sup>a</sup> Multiplied by  $\sqrt{2}$ .

<sup>b</sup> Multiplied by 2.

other octahedra may be permitted, independent of symmetry. Applying such a disordered model to the structural refinement of  $\text{Sr}_2\text{RhO}_4$ , we obtained smaller  $R$  values,  $R_{\text{wp}} = 13.17\%$ ,  $R_p = 9.34\%$ ,  $R_R = 11.35\%$ ,  $R_E = 3.46\%$ ,  $R_1 = 2.85\%$ , and  $R_F = 2.75\%$ . The results of structural refinement is given in Table 1. The occupation factors for O2(a) and O2(b) imply that the crystal statistically exhibits a partial disordering with respect to the rotation of  $\text{RhO}_6$  octahedra. When the occupation factor  $g$  is equal to 0.5 for O2(a) and O2(b) sites, disordering of the rotation of the  $\text{RhO}_6$  octahedra in the clockwise and counterclockwise directions occurs; thereby the crystallographic space group for  $\text{Sr}_2\text{RhO}_4$  changes to  $I4/mmm$ , as observed for  $\text{Sr}_3\text{Ir}_2\text{O}_7$  (11). In  $\text{Sr}_3\text{Ir}_2\text{O}_7$ , the angle of Ir–O–Ir in the  $\text{IrO}_2$  plane is smaller than  $180^\circ$ . Further discussion on the structural refinement was impossible since X-rays are insensitive to the position of oxygen ions. The above results indicate that  $\text{Sr}_2\text{RhO}_4$  has the same structure as  $\text{Sr}_2\text{IrO}_4$ , with space group  $I4_1/acd$ , i.e., the  $c$  axis length must be doubled and the  $a$  axis length must be multiplied by  $\sqrt{2}$ . In  $\text{Sr}_2\text{RhO}_4$ , the  $\text{RhO}_6$  octahedra rotates by  $10^\circ$  about the crystallographic  $c$  axis, while the rotating angle of  $\text{IrO}_6$  in  $\text{Sr}_2\text{IrO}_4$  is  $10.5^\circ$ . Figure 2 shows the  $\text{RhO}_2$  layers along the  $c$  axis for  $z = 1/8$  and  $3/8$ .

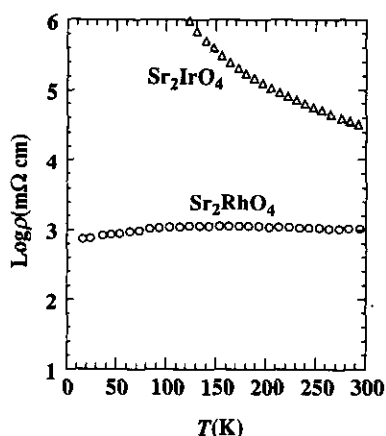


FIG. 4. Temperature dependence of the electrical resistivities for  $\text{Sr}_2\text{RhO}_4$  and  $\text{Sr}_2\text{IrO}_4$ .

Figure 3 shows the magnetic susceptibility for  $\text{Sr}_2\text{RhO}_4$  (4) and  $\text{Sr}_2\text{IrO}_4$  (11). Antiferromagnetic behavior can be observed for  $\text{Sr}_2\text{IrO}_4$  (12), but we did not observe any magnetic hysteresis for  $\text{Sr}_2\text{RhO}_4$  even at 5 K (4). Since the low-spin  $\text{Rh}^{4+}$  ion has the spin  $1/2$ , as does  $\text{Ir}^{4+}$ , the magnetic structure for single crystalline  $\text{Sr}_2\text{RhO}_4$  should be determined by neutron diffraction or by the muon spin rotation technique. Figure 4 shows the electrical resistivities for  $\text{Sr}_2\text{RhO}_4$  (4),  $\text{Sr}_2\text{IrO}_4$  (11).

Table 2 compares the crystallographic parameters for  $\text{Sr}_2\text{RhO}_4$ ,  $\text{Sr}_2\text{RuO}_4$  (12), and  $\text{Sr}_2\text{IrO}_4$  (13). The structural analysis data for  $\text{Sr}_2\text{IrO}_4$  was obtained by the powder neutron diffraction technique. Elongation of the Ru–O distance along the  $c$  axis is clearly observed in these compounds. The elongation is largest in  $\text{Sr}_2\text{RuO}_4$ ,  $d_{\text{Ru-O}(c)}/d_{\text{Ru-O}(a)} = 1.070$ , this value being considered to have originated from the cooperative Jahn–Teller distortion of high-spin  $\text{Ru}^{4+}$  ions (12). The values for  $\text{Sr}_2\text{RhO}_4$  and  $\text{Sr}_2\text{IrO}_4$  are almost the same; the  $t_{2g}^5$  electronic configuration in  $\text{Rh}^{4+}$  and  $\text{Ir}^{4+}$  leads to the same distortion of the  $\text{MO}_6$  octahedra, although the Rh and Ir belong to the second and third transition metals, respectively.

In conclusion,  $\text{Sr}_2\text{RhO}_4$  and  $\text{Sr}_2\text{IrO}_4$  have the same structure. It is to be noted that  $\text{Rh}^{4+}$  and  $\text{Ir}^{4+}$  have almost same ionic radii, 0.620 and 0.625 nm (15), respectively, and it can be recognized in the lattice parameters and interionic distances, as shown in Table 2. The explanation for the difference in the properties is not simple because the structures for  $\text{Sr}_2\text{RhO}_4$  and  $\text{Sr}_2\text{IrO}_4$  are almost same, including the rotating angles of  $\text{RhO}_6$  and  $\text{IrO}_6$ . The following two factors are considered to affect the properties of these two compounds: (a) a difference in size of the  $4d$  and  $5d$  electron orbitals of  $\text{Rh}^{4+}$  and  $\text{Ir}^{4+}$  ions and (b) differences in the energy levels for  $\text{O}2p$ ,  $\text{Rh}4d$ , and  $\text{Ir}5d$ . These factors definitely determine the properties of these two compounds and the itinerant or localized states of the electron.

#### ACKNOWLEDGMENT

The authors express their thanks for a Grant-in-Aid for Scientific Research, "Science of New Superconductors," from the Ministry of Education, Science, and Culture.

## REFERENCES

1. I-S. Kim, T. Nakamura, M. Itoh, and Y. Inaguma, *Mater. Res. Bull.* **28**, 1029 (1993).
2. T. Nakamura, T. Shimura, M. Itoh, and Y. Takeda, *J. Solid State Chem.* **103**, 523 (1993).
3. T. Shimura, M. Itoh, and T. Nakamura, *J. Solid State Chem.* **98**, 198 (1992).
4. T. Shimura, M. Itoh, Y. Inaguma, and T. Nakamura, *Phys. Rev. B* **49**, 5591 (1994).
5. C. N. R. Rao, P. Ganguly, K. K. Singh, and R. A. Mohan Ram, *J. Solid State Chem.* **72**, 14 (1988).
6. M. K. Crawford, M. A. Subramanian, R. L. Harlow, J. A. Fernandez-Baca, Z. R. Wang, and D. C. Johnson, *Phys. Rev. B* **49**, 9198 (1994).
7. F. Izumi, H. Murata, and N. Watanebe, *J. Appl. Crystallogr.* **20**, 411 (1987).
8. M. E. Leonowicz, K. R. Poppelmeier, and J. M. Longo, *J. Solid State Chem.* **59**, 71 (1985).
9. Q. Huang, J. L. Soubeyroux, O. Chmaissem, I. Nataki Sora, A. Santoro, R. J. Cava, J. J. Krajewski, and W. F. Pech, Jr., *J. Solid State Chem.* **112**, 355 (1994).
10. M. A. Subramanian, M. K. Crawford, and R. L. Harlow, *Mater. Res. Bull.* **28**, 645 (1994).
11. T. Shimura, Y. Inaguma, M. Itoh, and T. Nakamura, "Proceedings, 6th Int. Nat. Symp. Supercon., 1994," p. 275.
12. H. K. Müller-Buschbaum and J. Wilkens, *Z. Anorg. Allg. Chem.* **591**, 161 (1990).
13. T. Shimura, M. Itoh, and Y. Morii, unpublished work.
14. R. D. Shannon, *Acta Crystallogr. A* **32**, 751 (1976).